Structural environements around molybdenum in silicate glasses and melts. II. Effects of temperature, pressure, H2O, halogens and sulfur.

François Farges, Ralf Siewert, Carl W. Ponader, Gordon E. Brown Jr, Michel Pichavant, Harald Behrens

HAL Id: hal-00081785

https://hal-insu.archives-ouvertes.fr/hal-00081785

Submitted on 25 Sep 2020

STRUCTURAL ENVIRONMENTS AROUND MOLYBDENUM
IN SILICATE GLASSES AND MELTS. II. EFFECT OF TEMPERATURE, PRESSURE, H_2O, HALOGENS AND SULFUR

FRANÇOIS FARGES[§] AND RALF SIEWERT

*Laboratoire de Minéralogie (USM 201), Muséum National d'Histoire Naturelle, CNRS UMR 7160, 61, rue Buffon, F-75005
Paris, France, and Department of Geological and Environmental Sciences, Stanford University,
Stanford, California 94305-2115, USA*

CARL W. PONADER[¶] AND GORDON E. BROWN JR.

*Department of Geological and Environmental Sciences, Stanford University, Stanford, California 94305-2115,
and Stanford Synchrotron Radiation Laboratory, 2575 Sand Hill Road, MS 99, Menlo Park, California 94025, USA*

MICHEL PICHAVANT

*Institut des Sciences de la Terre d'Orléans (ISTO) – CRSCM–CNRS, 1A, rue de la Férollerie,
F–45071 Orléans Cedex 2, France*

HARALD BEHRENS

Institut für Mineralogie, Hannover Universität, Welfengarten 1, D–30167 Hannover, Germany

ABSTRACT

The local structure around molybdenum (at a concentration of 2000 ppm) in densified silicate glasses (to 7 kbar), melts (to 1210 K), and fluid-bearing (either H_2O, halogens, or sulfur) glasses was investigated by the means of X-ray absorption fine structure (XAFS) spectroscopy at the molybdenum K-edge. The spectra show that molybdate moieties [*i.e.*, $Mo(VI)O_4^{2-}$] are the dominant form of molybdenum in anhydrous melts and in densified glasses, with only a minor amount of tetravalent molybdenum. Also, H_2O and halogens have a limited effect on the local structure of molybdenum by promoting tetravalent coordination, but they do not complex Mo. In contrast, sulfur is found to complex molybdenum at moderate oxygen and sulfur fugacities. Thio-oxo-molybdate moieties [$Mo(IV,V,VI)O_nS_n$ (n = 1, 2, 3)] are observed in sulfur-bearing glasses. Thio-oxo-molybdate moieties are characterized by $Mo=S^{2-}$ bonds, which result in these moieties being disconnected (mobile) within the melt. These moieties also polymerize with decreasing redox state of Mo (as Mo–S units), enhancing molybdenite saturation and nucleation in the melt. A new and largely unexplored area of research involving the structure and stability of thio-molybdate moieties in magmatic systems is outlined, which can help reconcile some of the apparent discrepancies in the geochemistry of molybdenum in synthetic systems *versus* natural systems, in particular in systems where molybdenum partitions into the fluid phase.

Keywords: molybdenum, glasses and melts, XAFS spectroscopy, fluids, sulfur.

SOMMAIRE

La structure locale *in situ* autour du molybdène dans des verres densifiés (jusqu'à 7 kbar), des magmas (jusqu'à 1210 K), et dans des verres dopés en fluides (H_2O, halogènes ou soufre) a été caractérisée par spectrométrie d'absorption X au seuil K du molybdène. Le molybdate [Mo(VI)] est dominant dans les silicates fondus [le Mo(IV) représentant au plus un quart du molybdène], tout comme dans les verres densifiés (avec ou sans fluides). De plus, H_2O et halogènes ont un effet limité sur la spéciation du molybdène: apparition de Mo(IV) et absence de complexation directe. Au contraire, le soufre complexe efficacement le molybdène *via* des entités mixtes thio-molybdate [$Mo(IV,V,VI)O_nS_n$ (n = 1, 2, 3)]. Ces entités, contrairement à la molybdénite, possèdent des liaisons Mo=S et apparaissent à des fugacités de soufre elevées et des fugacités d'oxygène faibles. Les liaisons $Mo=S^{2-}$ maintiennent ces entités thio-molybdatées déconnectées (et donc mobiles) au sein du magma. Ces unités se polymérisent

---

[§] *E-mail address*: francoisfarges@gmail.com
[¶] *Present address*: Corning Inc., Sullivan Park, Corning, New York 14831, USA

quand la redox du molybdène décroît, favorisant la saturation en molybdénite (liaisons Mo–S simples) depuis le magma. Un nouveau domaine de la géochimie des entités thio-molybdatés de molybdène est mis en évidence dans les systèmes magmatiques, qui aide à réconcilier les informations structurales obtenues pour les magmas synthétiques avec les connaissances géochimiques, notamment où le molybdène se répartit vers les phases fluides hydrothermales.

Mots-clés: molybdène, verres, magmas, spectroscopie XAFS, fluides, soufre.

INTRODUCTION

In a companion paper (Farges *et al.* 2006), we established that molybdenum occurs dominantly as molybdate moieties [Mo(VI)O_4^{2-}] in a variety of anhydrous silicate glasses with variable composition (including variable polymerization of tetrahedra), even at relatively low fugacities of oxygen (as low as QFM–2 or ~10^{-9} atm at 1300°C and 1 bar). At even lower fugacities of oxygen (between IW and IW–1 or ~$10^{-10.5}$ atm at 1350°C and 1 bar), Mo(V) is the most abundant redox state of molybdenum. These results are at variance with previous models of the solubility of molybdenum in silicate melts (Holzheid *et al.* 1994, Walter & Thibault 1995, O'Neill & Eggins 2002); these investigators did not consider this redox state of molybdenum [as well as Mo(III)]. Under more reducing conditions, Mo(IV) is present only within the buffer range of IW–1 and IW–3. Under highly reducing conditions (*i.e.,* below IW–3), metallic molybdenum precipitates directly from the melt phase. No evidence for Mo(III) was found in any of the oxide glasses investigated by Farges *et al.* (2006). This information on the speciation of molybdenum suggests that Mo(VI) is the dominant redox state of molybdenum over a broad range of f(O$_2$) (air to IW–1). These findings appear to be at variance with the observed geochemistry of molybdenum in relatively oxidizing subvolcanic environments (such as in porphyry-type deposits), in which molybdenite [*i.e.,* a Mo(IV) sulfide] is the dominant molybdenum-bearing mineral (*e.g.,* Candela & Holland 1986, Carten *et al.* 1993, Bookstrom 1999).

In this study, we examine the influence of pressure on the speciation of molybdenum in densified silicate glasses and, in separate experiments, the influence of temperature on molybdenum speciation in silicate melts at temperature using XAFS spectroscopy, including both the X-ray absorption near-edge structure (XANES) and the extended X-ray absorption fine structure (EXAFS) regions. In addition, the influence of volatiles (including H$_2$O, fluorine, chlorine, and sulfur) is examined to better understand their effects on the local environment of molybdenum in these silicate glasses.

BACKGROUND INFORMATION

In order to develop a more comprehensive understanding of the speciation of molybdenum in magmatic systems, the effect of temperature, pressure, and volatile elements (such as H$_2$O, halogens, and sulfur) must be considered. Changes in local structure occur at temperatures above the glass transition (T$_g$) around divalent 3d transition elements such as Fe and Ni in dry and anhydrous melts (see Waychunas *et al.* 1988, Jackson *et al.* 1993, Farges *et al.* 1994, 2001, Brown *et al.* 1995, Berry *et al.* 2003), in contrast to highly charged cations (or high-field-strength, HFS, cations) such as titanium and zirconium, where little change in local structure is observed (see Farges *et al.* 1996, Farges & Rossano 2000). On the other hand, moderate pressure (to 7 kbar) is not expected to have a significant influence on the speciation of HFS cations [see Paris *et al.* (1994), Farges & Rossano (2000) for titanium and zirconium, respectively]. For example, the influence of relatively high pressure (50 kbar) and high temperature on the local environment of zirconium in H$_2$O-bearing synthetic and natural glasses is limited to a severe radial distortion of the ZrO$_6$ moieties, which is not easily quenchable (Farges *et al.* 2005).

In contrast, volatile constituents (such as H$_2$O, halogens) are considered to play a significant role in the speciation and transport of metal cations (see, among others, Keppler & Wyllie 1990, Linnen 1998, Horng 1999, Salova *et al.* 1989), particularly in the case of molybdenum (Isuk & Carman 1981, 1983, 1984, White *et al.* 1981, Candela & Holland 1984, Tingle & Fenn 1982, 1984, Keppler & Wyllie 1990, Chevychelov & Chevychelova 1997, Bai & Koster van Groos 1999, Schäfer *et al.* 1999, Webster 1999, Kravchuk *et al.* 2000, Seedorff & Einaudi 2004). Although H$_2$O, Cl (as NaCl), and CO$_2$ have been shown to have a dramatic effect on melt–fluid partitioning of molybdenum (Candela & Holland 1984, Tingle & Fenn 1984, Keppler & Wyllie 1990), the effect of fluorine is less important, except where large quantities of NaF are added to the melt (Bai & Koster van Groos 1999). However, the fact that volatiles enhance melt–fluid partitioning of molybdenum does not necessarily mean that molybdenum is complexed by these volatiles in all cases. For instance, no direct complexation of Zr, Th, and U by H$_2$O, F, or Cl was observed in XAFS spectroscopy studies of fluid-bearing glasses (Farges 1991, Farges *et al.* 1991, 1992, Farges & Rossano 2000). However, these authors reported that structural depolymerization induced by the presence of fluids in the melt plays a key (albeit indirect) role in affecting the solubility of metal cations, especially in highly polymerized melts synthesized in equilibrium with H$_2$O (see also Kohn 2000).

Finally, the influence of sulfur on the speciation of molybdenum in silicate glasses of geochemical interest is not well known. According to Tingle & Fenn (1982, 1984), sulfur has no direct effect on molybdenum melt–fluid partitioning, but it does play a critical role in the deposition of molybdenum from the vapor phase. The influence of sulfur on the speciation of molybdenum in silicate glasses of geochemical interest is not well known. According to Tingle & Fenn (1982, 1984), sulfur has no direct effect on molybdenum melt–fluid partitioning, but it does play a critical role in the deposition of molybdenum from the vapor phase. Tingle & Fenn (1984) also concluded that the initial H_2O content of the magma (which controls the timing of evolution of the vapor phase) and the presence of sulfur are the primary controls on molybdenum ore deposition in porphyry-type deposits. In parallel, Isuk & Carman (1983, 1984) concluded from their experiments that molybdenum ["possibly as $MoSi_2O_4(OH)^{3+}$ complexes"] and sulfur fractionate strongly into the vapor phase, where these two elements recombine as molybdenite because of the chalcophile character of molybdenum under subvolcanic conditions. In addition to its effect on the geochemical behavior of molybdenum, sulfur is also known to affect some of the optical and chemical properties of industrial oxide glasses (as for the "dead leaf" pigment or for molybdenum oxi-sulfide-based glasses, which are used for hydro-cracking catalysis: Bensimon et al. 1991).

<center>EXPERIMENTAL</center>

Synthesis of glass samples

"High-pressure" glasses (to 7 kbar) were synthesized from homogenized Mo-doped glasses using an internally heated pressure vessel (IHPV). Details on sample preparation and characterization can be found in Farges et al. (2001). Conditions of synthesis are summarized in Table 1. Hydrous glasses were H_2O-saturated (Ab) or nearly so (NS3). Their final H_2O contents were determined by Karl–Fisher titrations and infrared (IR) spectroscopy measurements (Table 2). The initial quench-rate in the IHPV was around 200 K/min. In the range of the glass-transition temperature (600 to 1100 K, depending on anhydrous composition and H_2O content), the cooling rate of the samples in the IHPV decreases to 50 to 100 K/min. Fluorine- and chlorine-bearing glasses were synthesized at 0.5 kbar using the protocol described in Ponader & Brown (1989a, b). As for the IHPV-synthesized samples, the oxygen fugacity was not precisely measured during the synthesis of the F- and Cl-bearing glasses (intrinsic conditions, Ar atmosphere). However, on the basis of measurements of U-redox equilibria in silicate melts performed in the same furnace, we estimate that the conditions are QFM–1 (±1) log units of $f(O_2)$ (1750 K and 500 bars; Farges et al. 1992). The intrinsic fugacity conditions are

mostly controlled by the fugacity of hydrogen (which is related to the H_2O content of the sample because of the dissociation of water). Finally, sulfur-bearing glasses were prepared in a gas-mixing furnace at 1 atm. Fugacities of gaseous species [$f(O_2)$, $f(S_2)$] were controlled by the composition of a $CO–CO_2–SO_2$ gaseous mixture. A zirconia cell was used to measure $f(O_2)$ directly. More details on the preparation of the sulfur-rich glasses can be found in Azif (1998). The experimental conditions for the glasses of that study are presented in Table 1. Chemical compositions of the glasses after synthesis are within 1 mol.% of their nominal values (Table 2). The glasses of albite composition (Ab) quenched from pressures above 1 bar do show some increase in density, whereas the H_2O-bearing ones show a decrease in density by at most 2% (at 7 kbar), suggesting that their high-pressure structure was at least partially quenched.

The collection and analysis of XAFS data

XAFS spectra were collected on beamlines 4–1 and 4–4 at the Stanford Synchrotron Radiation Laboratory (Stanford, California), as described in Farges et al.

TABLE 1. CONDITIONS OF SYNTHESIS OF THE GLASS SAMPLES

Run no.	sample	Mo (ppm)	T (K)	P (bar)	atmos-phere	$f(O_2)$ (buffer)	duration (hrs)
6a	NS2	1000	1104	1	air	- 0.7	6
6b	NS2	12000	1104	1	air	- 0.7	6
27	Ab (2.5 kbar)	2000	1650	2500	intrinsic	NNO-1	24
28	Ab (5 kbar)	2000	1650	5000	intrinsic	NNO-1	24
29	Ab (7 kbar)	2000	1650	7000	intrinsic	NNO-1	24
30	Ab (hydrous)	2000	1650	7000	intrinsic	NNO+3	24
31	$Ab_{50}An_{50}$ (dry)	2000	1650	7000	intrinsic	NNO-1	24
32	$Ab_{50}An_{50}$ (hydrous)	2000	1650	7000	intrinsic	NNO+3	24
33	$Ab_{30}An_{70}$ (dry)	2000	1650	7000	intrinsic	NNO-1	24
34	$Ab_{30}An_{70}$ (hydrous)	2000	1650	7000	intrinsic	NNO+3	24
35	NS3 (hydrous)	2000	1650	7000	intrinsic	NNO+3	24
40	NS3	2000	1750	500	intrinsic	~ QFM-1	8
41	NS3+F	2000	1750	500	intrinsic	~ QFM-1	8
42	NS3+Cl	2000	1750	500	intrinsic	~ QFM-1	8
43	Pr	2000	1750	500	intrinsic	~ QFM-1	8
44	Pr+F	2000	1750	500	intrinsic	~ QFM-1	8
45	Pr+Cl	2000	1750	500	intrinsic	~ QFM-1	8
46	Ab	2000	1750	500	intrinsic	~ QFM-1	8
47	Ab+F	2000	1750	500	intrinsic	~ QFM-1	8
50	NS2	2000	1650	1	$CO-CO_2-SO_2$	~ QFM-1	8
51	NS2	2000	1650	1	$CO-CO_2-SO_2$	~ IW	8
52	NS2	2000	1650	1	$CO-CO_2-SO_2$	~ IW-1	8
53	NS3	2000	1650	1	$CO-CO_2-SO_2$	~ QFM-1	8
54	NS3	2000	1650	1	$CO-CO_2-SO_2$	~ IW	8
55	NS3	2000	1650	1	$CO-CO_2-SO_2$	~ IW-1	8

Note: the so-called "intrinsic" conditions (using Ar) were determined from a comparison of the spectra obtained here with those presented in Farges et al. (2006). At intrinsic conditions in the IHPV facility, the hydrogen fugacity (near 1 bar) corresponds to an oxygen fugacity close to NNO + 3 if the capsule is H_2O-saturated (Wilke & Behrens 1999, Berndt et al. 2002), but conditions are more reducing (~NNO–1) at lower content of H_2O (reaction $H_2 + \frac{1}{2} O_2 = H_2O$). These conditions of oxygen fugacity were also consistent (at ±1 log unit) with other experiments conducted with U-bearing glasses (Farges et al. 1992).

(2006). All XAFS data were collected under high-resolution conditions between 1995 and 1997 (SPEAR2 storage ring), except for the halogen-bearing glasses, for which XAFS data were collected in 1985 under low-resolution conditions. *In-situ* high-temperature XANES and EXAFS spectra were collected using a heating loop furnace working in the fluorescence-yield mode [see Farges *et al.* (1996) for details]. All EXAFS spectra were collected at ambient temperature. The EXAFS spectra were analyzed using the cumulant expansion formalism (Crozier *et al.* 1988), which is reliable for low to moderate degrees of anharmonicity. If anharmonicity is not accounted for in such spectra, the EXAFS-derived interatomic distances and coordination numbers may be significantly underestimated [see Brown *et al.* (1995) for details] and would conflict with structural information derived from XANES pre-edge spectra, which are not affected by anharmonicity. Because of the high charge of molybdenum in these melts, Mo–O bonds are highly covalent (Ozeki *et al.* 1996) and exhibit little thermal expansion. Consequently, these bonds are not predicted to have significant anharmonicity (Brown

et al. 1995). In the present study, we used the same software package for analysis of EXAFS data ("xafs 2.6"; Winterer 1997) as that we used in the companion study (Farges *et al.* 2006). The reader is referred to that article for further details on EXAFS data analysis. In some compositions of polymerized melt (such as the anhydrous feldspathic ones), significant asymmetry in the Mo–O pair distribution function was detected, which apparently shifts the main Mo–O peak in the FT to lower (R + ΔR) values. The refined ΔE_0 parameter tends to zero values (±5 eV), which is the actual core-hole lifetime at the molybdenum K-edge (Krause & Oliver 1979). In some cases, higher ΔE_0 values (the edge-energy shift, E_0, as compared to the model, which is a fit-quality factor that should be as close to zero as possible) were obtained (Table 3). To address this problem, we used a variety of experimental and theoretical phase-shifts, which we think is related to the poor transferability of phase-shifts from molybdate units (as in sodium molybdate dihydrate) to more reduced and much less covalent M–O bonds [such as for Mo(IV)]. However, we did not find a suitable model compound for Mo(IV)–O bonds, in which the local structure is sufficiently radially ordered so that we could extract reliable amplitudes and phase-shifts for the Mo(IV)–O pair. Consequently, the relatively high values of ΔE_0 remain in some of the models presented here.

RESULTS

Effect of temperature (*in situ*)

Figure 1a shows high-resolution XANES spectra collected at the molybdenum K-edge for two NS2 compositions (containing 1.2 and 0.102 wt.% molybdenum, respectively) to 1210 K. Conditions of synthesis for these two glasses were given in Table 1 of Farges *et al.* (2006, sample 6a). The XANES spectra show an intense pre-edge feature, suggesting the presence of dominant amounts of molybdate units, *i.e.*, $Mo(VI)O_4^{2-}$ (Farges *et al.* 2006). This feature also is present well above the glass-transition temperature, T_g of NS2 (~600 K). The edge crest shows significant broadening due to high thermal disorder in the melt. However, the main features of the XANES spectra (including the electronic transitions resulting in the pre-edge feature) have the same energy position over the temperature range studied. Figure 2 shows the pre-edge information derived from the molybdenum K-edge XANES, using the template of Figure 3b of Farges *et al.* (2006). The pre-edge information confirms the presence of dominant amounts of molybdate moieties in these melts to 1210 K. Changes in temperature (295–1210 K range) and in molybdenum concentration (1020–12000 ppm range) do not affect molybdenum speciation in these samples. Similar results (not presented) were obtained for sodium trisilicate and glass and melts of albite composition

TABLE 2. COMPOSITIONS OF THE GLASSES STUDIED

composition	SiO$_2$	Al$_2$O$_3$	CaO	Na$_2$O	F, Cl	MoO$_3$	SO$_3$	H$_2$O*	Σ
Ab (2.5 kbar)	68.9	18.8		12.2		0.28			100.2
Ab (5 kbar)	69.0	18.7		12.0		0.25			100.0
Ab (7 kbar)	69.1	19.1		11.7		0.16		0.16	100.2
Ab (hydrous)	63.0	17.2		10.5		0.20		8.10	99.0
Ab$_{50}$An$_{50}$ (dry)	54.8	28.6	10.2	5.9		0.27		0.02	99.8
Ab$_{50}$An$_{50}$ (hydrous)	51.3	26.0	9.4	5.6		0.38		7.35	100.0
Ab$_{30}$An$_{70}$ (dry)	50.4	31.6	14.0	3.7		0.15		0.01	99.9
Ab$_{30}$An$_{70}$ (hydrous)	46.4	28.0	12.9	3.3		0.25		7.97	98.8
NS3 (hydrous)	71.8			19.5		0.23		8.20	99.7
NS3	74.1	0.1		25.9		0.21			100.3
NS3+F	73.2	0.1		24.5	2.1	0.23			100.1
NS3+Cl	72.6	0.1		24.8	0.6	0.24			98.3
Pr**	73.3	9.1		17.9		0.16			100.5
Pr+F**	70.3	9.2		17.7	2.8	0.23			100.2
Pr+Cl**	71.2	9.5		17.9	0.6	0.17			99.4
Ab	69.2	19.4		11.5		0.25			100.4
Ab+F	67.7	18.5		12.5	1.9	0.19			100.8
NS2 $f(O_2) = 10^{-8.0}$ $f(S_2) = 10^{-1.6}$	72.0			23.9		0.11	2.40		98.4
NS2 $f(O_2) = 10^{-10.2}$ $f(S_2) = 10^{-1.6}$	72.2			23.4		0.09	2.30		98.0
NS2 $f(O_2) = 10^{-11.1}$ $f(S_2) = 10^{-1.6}$	70.4			27.8		0.12	2.75		101.1
NS3 $f(O_2) = 10^{-8.0}$ $f(S_2) = 10^{-1.6}$	75.5			24.4		0.12	0.80		100.8
NS3 $f(O_2) = 10^{-10.2}$ $f(S_2) = 10^{-1.6}$	76.1			24.1		0.13	0.80		101.1
NS3 $f(O_2) = 10^{-11.1}$ $f(S_2) = 10^{-1.6}$	75.6			23.8		0.10	0.79		100.3

* measured by infrared spectroscopy: for the low H$_2$O contents at 3550 cm^{-1}, and for the high H$_2$O contents near 4500 cm^{-1} (OH band) and near 5200 cm^{-1} (H$_2$O band). ** Pr is a composition "half-way" between albitic (Ab) and sodium trisilicate (NS3) compositions. Other acronyms include sodium disilicate (NS2) and anorthitic (An). The compositions, expressed in weight percent, were established by electron-microprobe analysis.

exposed to similar conditions of temperature (T_g is ~1250 K for the Mo-free albitic composition).

Effect of pressure during synthesis

High-resolution molybdenum K-edge XANES for glasses of albite composition (Ab) quenched from moderate pressures (to 7 kbar) are presented in Figure 1b. Their molybdenum K-edge pre-edge information also is shown in Figure 2. The intrinsic oxygen fugacity conditions for these experiments are NNO–1 (see Table 1 for details) under dry conditions (Wilke & Behrens 1999, Berndt *et al.* 2002). These conditions are reducing enough to produce a brownish color for these glasses, which is typical of Mo(V), as described in Farges *et al.* 2006. This reduction in the oxidation state of molybdenum is possibly related to the low fugacity of H_2O in these experiments (nominally anhydrous but, in reality, slightly hydrous), which tends to increase slightly [~1/2 log units of $f(O_2)$] the oxygen fugacity at a given intrinsic condition. However, following Farges *et al.* (2006), these intrinsic conditions do not significantly affect the average redox state of molybdenum in anhydrous glasses, which remains mostly as Mo(VI). The XANES spectra for the densified glasses show no significant changes compared to their counterparts synthesized at 1 bar; the intense pre-edge feature indicates dominant amounts of molybdate moieties. However, the pre-edge information for these glasses (see Fig. 2) shows that minor amounts of Mo(V) or Mo(IV) or both (*i.e.*, ~100 ppm or ~5 at.% of the total Mo) is present in these glasses, as a result of a slightly lower pre-edge height (~0.5 *versus* ~0.6 in the 1 bar Ab glass; Farges *et al.* 2006).

EXAFS spectra (and their best-fit models) are presented in Figure 3a, together with their Fourier Transforms (Fig. 3b). The structural parameters are in excellent agreement with those for molybdate moities [~4 atoms of oxygen at ~1.76 ± 0.01(1) Å]. However, to reduce the anomalously high ΔE_0 values during the modeling of these EXAFS spectra, a second shell of oxygen atoms was added [which converged to average Mo–O distances of 1.85(2) Å] (Table 3). Because of the very small difference in Mo–O distances (~0.1 Å), these longer bonds cannot graphically be resolved from the shorter ones in the FT. These longer Mo–O distances are typical of either 5-coordinated Mo(VI) or 4-coordinated Mo(IV) or both (based on effective ionic radii sums: Shannon & Prewitt 1969). These moieties cannot be identified more precisely because they are too dilute. The reduction of molybdenum during these high-pressure experiments is again confirmed by the brownish color of these densified glasses [indicative of Mo(V)]. In contrast, their 1 bar counterparts (synthesized in air) are translucent. Accordingly, longer Mo–O bonds were not detected in the glasses prepared at 1 bar pressure (Farges

TABLE 3. MOLYBDENUM K-EDGE EXAFS DATA-REDUCTION PARAMETERS FOR THE Mo–O PAIR FOR THE GLASSES INVESTIGATED

sample		shell	N	R (Å)	$\Delta\sigma^2$ (Å^2)	ΔE_0 [§]	χ^2 *
Ab (2.5 kbar) [§]		#1, O	3.8	1.78	0.006	+3.7	0.0029
		#2, O	0.5	1.83	0.007		
Ab (5 kbar) [§]		#1, O	3.8	1.77	0.006	+2.7	0.0033
		#2, O	0.9	1.83	0.007		
Ab (7 kbar) [§]		#1, O	3.9	1.78	0.007	+3.6	0.0022
		#2, O	0.6	1.84	0.008		
7 kbar glasses							
Ab (hydrous)		#1, O	3.7	1.77	0.004	+4.2	0.0011
		#2, O	0.7	1.94	0.005		
$Ab_{50}An_{50}$ (dry) [§]		#1, O	3.2	1.75	0.004	+3.0	0.0041
		#2, O	0.8	1.85	0.004		
$Ab_{50}An_{50}$ (hydrous)		#1, O	3.7	1.77	0.004	+5.2	0.0021
		#2, O	0.4	1.99	0.006		
$Ab_{30}An_{70}$ (dry) [§]		#1, O	3.3	1.75	0.005	+3.0	0.0013
		#2, O	1.1	1.85	0.004		
$Ab_{30}An_{70}$ (hydrous)		#1, O	3.7	1.75	0.003	+5.5	0.0017
		#2, O	0.3	1.94	0.005		
NS3 (hydrous)		#1, O	3.5	1.75	0.002	+4.5	0.0022
			0.9	1.98	0.007		
0.5 kbar glasses							
Ab [§]		#1, O	3.2	1.75	0.004	+4.4	0.0026
		#2, O	1.0	1.98	0.003		
Ab+F		#1, O or F	3.5	1.77	0.003	+6.5	0.0059
		#2, O	1.1	2.01	0.003		
NS3		#1, O	4.3	1.77	0.004	+6.6	0.0056
		#2, O	1.4	2.02	0.003		
NS3+F		#1, O or F	3.6	1.77	0.003	+6.8	0.0002
		#2, O or F	1.4	2.02	0.003		
NS3+Cl		#1, O	3.3	1.77	0.002	+7.2	0.0056
		#2, O	1.1	2.01	0.003		
Pr		#1, O	4.3	1.77	0.004	+6.5[†]	0.0055
		#2, O	1.5	2.02	0.003		
Pr+F		#1, O or F	3.6	1.77	0.003	+7.7[†]	0.0180
		#2, O or F	1.4	2.02	0.002		
Pr+Cl		#1, O	4.3	1.77	0.003	+5.8[†]	0.0081
		#2, O	1.5	2.02	0.003		
S-bearing glasses (1 atm)							
NS2	$f(O_2)$ = -8.0	#1, O	3.6	1.77	0.004	+0.2	0.0034
	$f(S_2)$ = -1.6	#2, S	–	–	–	–	
NS2	$f(O_2)$ = -10.2	#1, O	1.0	1.77	0.004	+0.5	0.0054
	$f(S_2)$ = -1.6	#2, S	2.8	2.15	0.008		
NS2	$f(O_2)$ = -11.4	#1, O	1.6	1.77	0.007	+0.3	0.0061
	$f(S_2)$ = -1.6	#2, S	2.0	2.14	0.010		
NS3	$f(O_2)$ = -8.0	#1, O	3.5	1.78	0.003	-0.2	0.0030
	$f(S_2)$ = -1.6	#2, S	–	–	–	–	
NS3	$f(O_2)$ = -10.2	#1, O	1.1	1.78	0.005	+0.4	0.0089
	$f(S_2)$ = -1.6	#2, S	2.6	2.18	0.005	+0.1	
NS3	$f(O_2)$ = -11.4	#1, O	1.5	1.77	0.010	+0.5	0.0102
	$f(S_2)$ = -1.6	#2, S	1.9	2.13	0.008	+0.2	
average error			0.5	0.02	0.001	1.0	

* Chi-square of the least-squares fit to the data.
[†] These values for ΔE_0 are due to the presence of a reduced oxidation state of molybdenum that cannot be modeled properly with amplitude and phases from sodium molybdate dihydrate (modeling with MoO_2 is even worse owing to disorder effects in that structure).
[§] Anharmonic contribution included (third cumulant, ~10^{-3} Å^{-3} not reported here).
Notes: Back-scattering amplitude- and phase-shifts from $Na_2MoO_4 \cdot 2H_2O$ (empirical) for all glasses, except for S-bearing glasses, in which cases FEFF8.2 functions were used, on the basis of the structure of $Cs_2Mo(VI)OS_3$ (Krebs *et al.* 1970). Anharmonic third-cumulant parameter (C^3) converged to zero for all models.
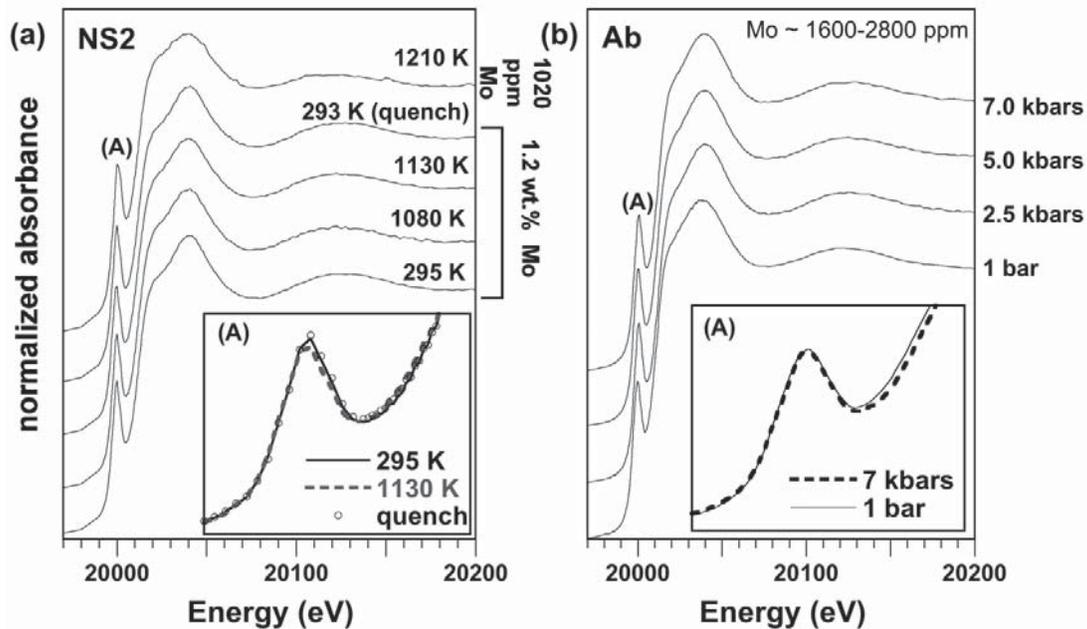
FIG. 1. (a) Molybdenum K-edge XANES spectra for a sodium disilicate (NS2) glass (containing 1.2 and 0.102 wt.% Mo) exposed (*in situ*) to 1210 K and quenched, showing the negligible effect of T_g on Mo(VI) speciation. (b) Mo K-edge XANES spectra for various densified glasses of albite (Ab) composition quenched from pressures to 7 kbar. The insets for both figures show the weak variations in pre-edge feature (feature A).
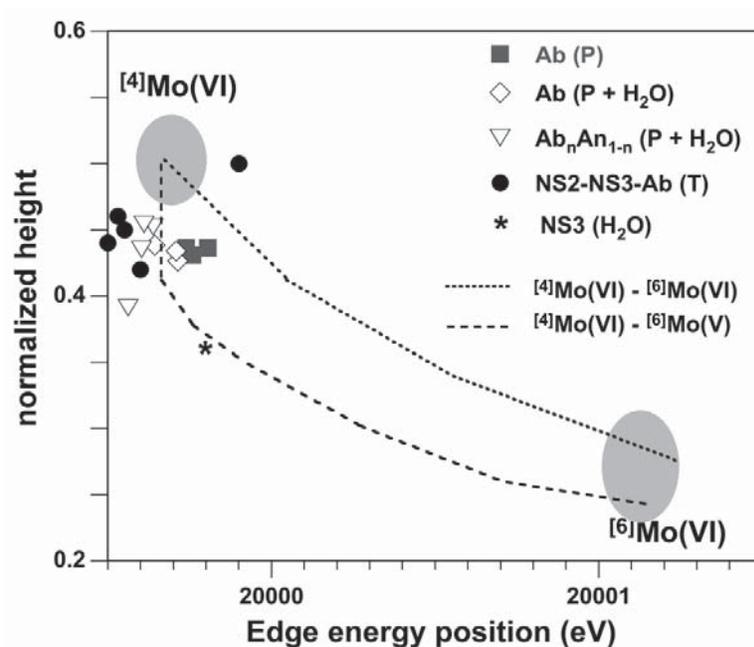

FIG. 2. Pre-edge information for the *in situ* (high-temperature, "T"), densified ("P") and H₂O-bearing glasses ("P+H₂O"), using the template from Figure 3b in Farges *et al.* (2006).

et al. 2006). We therefore conclude, on the basis of the XANES and EXAFS data, that the reducing conditions during the preparation of these high-pressure glasses induced a small but detectable amount of longer Mo–O bonds [typical of small amounts of Mo(V) or Mo(IV) or both]. This reduction aside, the 7 kbar pressure does not appear to cause significant contraction of the average Mo–O distance in molybdate moieties.

Effect of H_2O

High-resolution molybdenum K-edge XANES spectra for hydrous, high-pressure (6 kbar) feldspathic glasses (Ab and Ab_xAn_{1-x} with $x = 0.3$ and 0.5) are compared to their anhydrous (1 bar) counterparts in Figure 4a. There is no clear influence of H_2O on the local structure of these highly polymerized glasses. However, the XANES pre-edge information for the densified glasses suggests dominant amounts of molybdate units, together with some more highly coordinated environments around molybdenum. The EXAFS spectra for these glasses and their best-fit models are presented in Figure 5a, together with their Fourier Transforms (Fig. 5b). No quantitative difference in molybdenum speciation is observed as a function of both the matrix composition and H_2O content (see also Table 3);

however, a second shell of oxygen atoms was required to achieve a good fit, which indicates the presence of more highly coordinated molybdenum in addition to [4]Mo. The average Mo–O distance for this more highly coordinated species of molybdenum is much larger than that for the anhydrous counterparts (~1.94–1.99 Å as compared to 1.84–1.85 Å). Based on considerations of ionic radii (Shannon & Prewitt 1969), this average Mo–O distance is typical of 6-coordinated Mo(IV) environments. Hence, the presence of H_2O in these densified and relatively oxidized melts favors a higher coordination around Mo(IV). Similar conclusions are reached for the less polymerized, hydrous, high-pressure NS3 glass (Fig. 4b). In this glass, the molybdenum K-edge pre-edge feature is less intense and is shifted toward higher energies (see Fig. 2). Models of the EXAFS spectrum for the H_2O-saturated NS3 glass (Figs. 5a, b) suggest that two shells of oxygen atoms as first neighbors are also required to model the EXAFS spectra. The first shell (<Mo–O> ~1.75–1.77(2) Å) is clearly assignable to molybdate moieties. The slightly longer average Mo–O distances for the second oxygen shell (near 1.97–2.03 Å, see Table 3) suggest octahedrally coordinated Mo(IV), as in MoO_2 (Bendor & Shimony 1974). Accordingly, the pre-edge information suggests a 70:30 mixture of $Mo(VI)O_4^{2-}$ (molybdate)
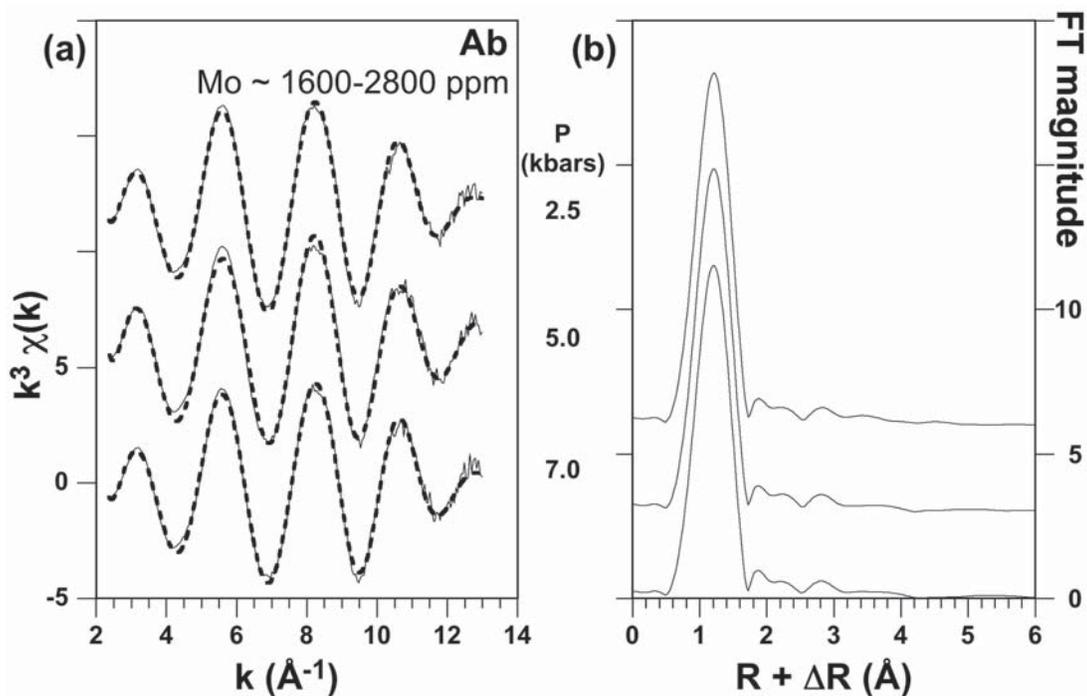

FIG. 3.   Molybdenum K-edge-normalized, k^3-weighted EXAFS spectra (a) (solid: experimental; dotted: calculated model) and their corresponding Fourier transforms (b) for three densified glasses of albite composition to 7 kbar.
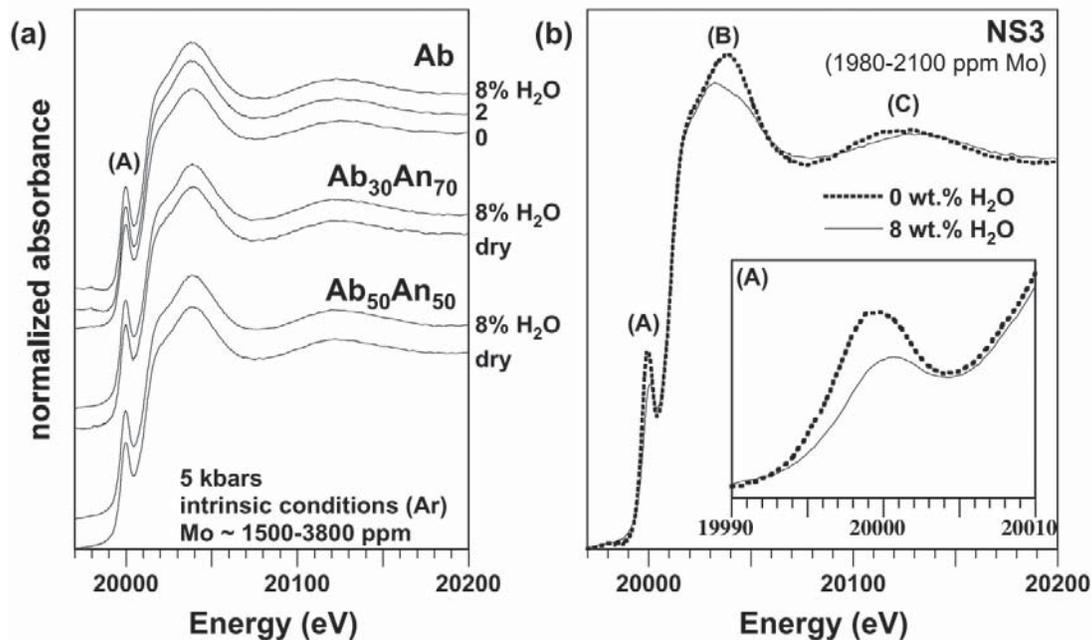
FIG. 4.   Molybdenum K-edge XANES spectra for dry and H₂O-bearing densified felsdpathic glasses (a) and sodium trisilicate glasses (b). Changes in the pre-edge feature (A) are observed only in NS3 glasses and are attributed to the presence of Mo(IV) moieties.
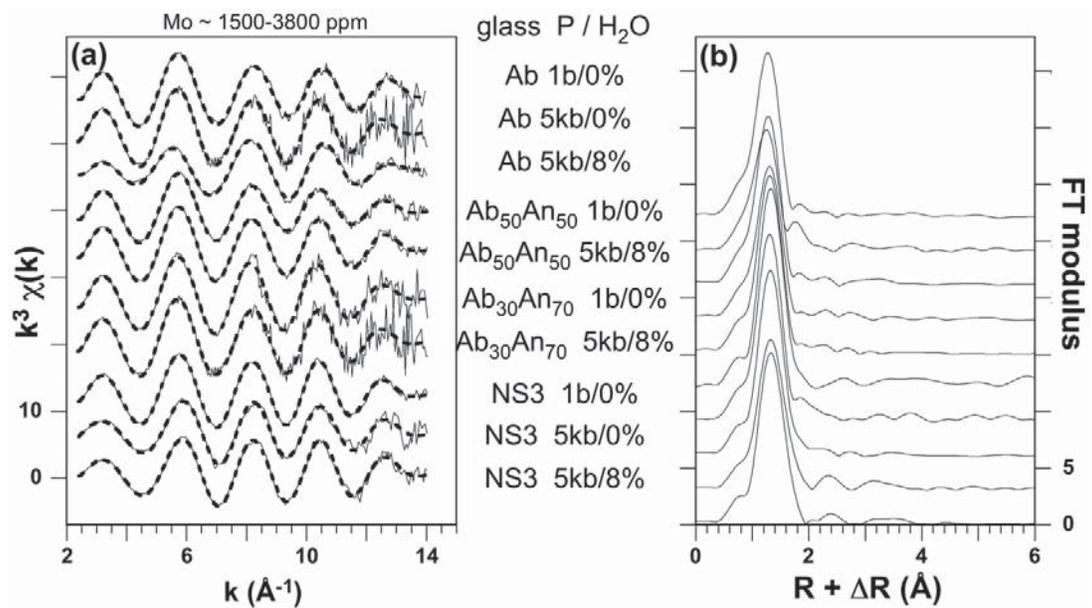

FIG. 5.   Molybdenum K-edge-normalized, k^3-weighted EXAFS spectra (a) (solid: experimental; dotted: calculated model) and their corresponding Fourier-transforms (b) for various dry and hydrous densified feldpathoidal and sodium trisilicate glasses. No splitting of features in the FT is observed for NS3 glasses, ruling out the presence of molybdenyl moieties in significant amounts in these glasses.

and Mo(IV)O$_6^{8-}$ units (see detailed information in Fig. 3b of Farges *et al.* 2006). The average oxidation state of molybdenum in that glass is 5.4. This redox information is also consistent with that inferred from the molybdenum K-edge position of NS3 glass (5.5 ± 0.02) or from the number of neighbors for each oxygen shell derived from EXAFS fitting [Table 3: 3.5(5) atoms of oxygen for Mo(VI) and 0.9(5) atoms of oxygen for Mo(IV) are consistent with an average redox of 5.6(3)]. However, as is the case for the densified glasses, the presence of minor or trace amounts of molybdenyl moieties [*i.e.,* Mo(V)] cannot be excluded in these glasses, as suggested by their brownish color.

Effect of halogens

Seven glasses (labeled "NS3", "Ab", and "Pr", the last being "half-way" between NS3 and Ab in composition; see Ponader & Brown 1989a, b, Farges *et al.* 1992) were prepared under the same conditions, with and without halogens (see Table 2 for compositions). The pre-edge spectra of these seven glasses (feature A in Fig. 6a) are relatively poorly resolved, owing to the conditions of low-energy resolution during data collection. As a result, the pre-edge A appears as a shoulder. Despite this limitation, the shoulder intensity and position are not affected by the presence of F or Cl in the three compositions investigated. Analysis of the edge position (which is much less sensitive to resolution than the pre-edge) for these glasses using the method described in Farges *et al.* (2006) suggests that the average state of oxidation of the molybdenum is constant in these seven glasses, between 5.5 and 6.0(5). Compared to their halogen-free counterparts, the edge-crest position for the halogen-bearing NS3 glasses (feature B in Fig. 6b) is slightly shifted toward lower energies. This observation suggests the presence of a distinct local structure of molybdenum in the F- and Cl-bearing glasses compared to their halogen-free counterparts. Finally, the first EXAFS oscillation for the halogen-bearing glasses (feature C in Fig. 6b) is located at the same energy position for all of these glasses, suggesting that oxygen ligands predominate around the molybdenum atom in all glasses, with comparable average Mo–O distances. However, feature C for the halogen-bearing glasses is less intense than for the halogen-free glasses, suggesting a more ordered environment in the halogen-free NS3 glasses. We
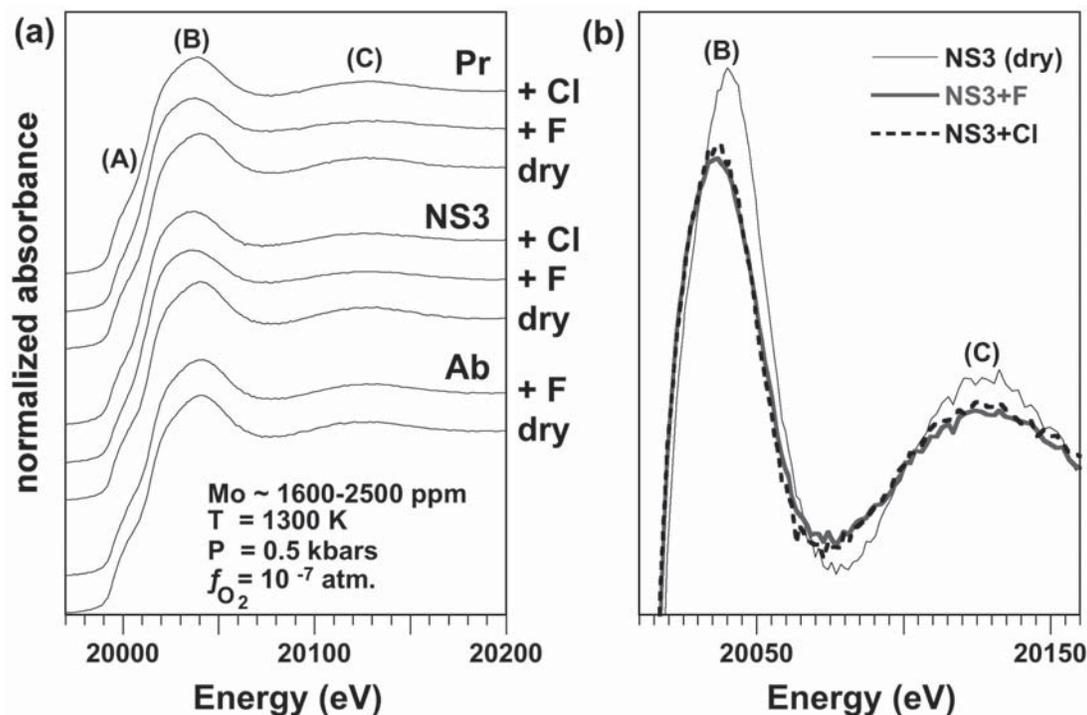

FIG. 6. (a) Molybdenum K-edge XANES spectra for three sets of slightly densified (0.5 kbar) glasses: sodium trisilicate ("NS3"), albitic ("Ab") and "peralkaline" ("Pr", which is compositionally "half-way" between NS3 and Ab). (b) Overlapped spectra for the three NS3 glasses of Figure 5a, and blown-up edge crest region (feature B) and the first EXAFS oscillation (feature C), whereas the pre-edge feature (A) is broadened.

found similar results for the two "Ab" and three "Pr" compositions investigated in this study. Therefore, the halogen-bearing glasses studied show very similar local environments of the molybdenum: similar average Mo–X distance (X being O, F or Cl) as the halogen-free glasses, except that the local environments of molybdenum are slightly more radially disordered in the presence of the halogens. However, because the local structure around molybdenum is different in the halogen-bearing and halogen-free glasses, the presence of halogen affects the Mo–O coordination environment (toward more radially distorted environments).

Identification of halogen ligands

Although the fluorine contents of the F-bearing glasses in this study are high enough to potentially complex all molybdenum atoms, the chlorine content (~6000 ppm; see Table 2) would result in "complexation" of, at most, half of the molybdenum atoms by chlorine as $Mo(VI)Cl_4^{2+}$ moieties. XAFS spectroscopy is much more sensitive to the presence of chlorine ligands than to oxygen ligands because of the much larger back-scattering amplitude of Cl (Farges *et al.* 1993). Because the molybdenum EXAFS spectra of Cl-free and Cl-bearing glasses examined in this study are very similar, we conclude that no detectable amount of chlorine (less than 5 at.% of the ligands around molybdenum) is located in the first coordination shell around molybdenum in the two Cl-bearing glasses ("Pr" and "NS3"). In contrast, the distinction between fluorine and oxygen ligands cannot be made using XAFS spectroscopy if based only on a simple analysis of the spectra because of the similar back-scattering amplitudes of oxygen and fluorine. However, the bonding requirements of fluorine are very different from those of oxygen (fluorine is monovalent, whereas oxygen is divalent), and their ionic radii differ by 0.07 Å (1.35 and 1.28 Å, respectively, for 2-coordinated oxygen and fluorine: Shannon & Prewitt 1969), which is well above the detection limits of XAFS (~0.02 Å). Therefore, replacement of oxygen by fluorine in the first coordination shell of molybdenum should result in a significant increase in the number of nearest neighbors and in average Mo–X distance (X: F or O or both) and, consequently, in the XAFS spectra (particularly in the pre-edge region) (see Cotton & Wilkinson 1988).

Thus, the EXAFS spectra for these glasses were modeled assuming oxygen first neighbors (Fig. 7a). Their Fourier Transforms (Fig. 7b) shows a Mo–O pair correlation for the most polymerized Ab glass that is shifted toward shorter Mo–O distances, as compared to the other glasses of this study (densified, hydrous and anhydrous). However, this shift is an artifact resulting from anharmonic effects due to asymmetric static disorder, related to the presence of some reduced molybdenum environments (Table 3). Accordingly, the oxygen environment around molybdenum is split into

two shells. The first oxygen shell (located near 1.75 Å) is related to molybdate moieties, whereas more distant first neighbors (near 2.00 Å) are related to a more highly coordinated form of molybdenum. As for the hydrous glasses, the longer Mo–O distance is typical of 6-coordinated Mo(IV). According to this model, Mo(IV) contributes to ~1/4 (atomic) of the molybdenum K-edge EXAFS signal. On the basis of this information, the average oxidation state of molybdenum in these seven glasses is 5.5, in agreement with information concerning their edge position. Hence, H_2O and chlorine affect the local structure of molybdenum in a very similar (but indirect) way, by promoting a slightly more disordered average local structure around molybdenum (as suggested by the XANES spectra) owing to the presence of Mo(VI) and Mo(IV) [and most likely Mo(V) as well].

Effect of sulfur

The high-resolution molybdenum K-edge XANES spectra for sulfur-free and sulfur-bearing NS2 and NS3 glasses (Figs. 8a and b, respectively) show large differences. Although the sulfur-free glasses show evidence of molybdate moieties (as a well-resolved pre-edge feature A), their sulfur-rich counterparts do not (see Fig. 8c; only a shoulder is detected in the pre-edge region), despite the fact that they were prepared at comparable fugacities of oxygen. However, these differences are related to changes in oxidation state of molybdenum as the edge position of these glasses shifts toward higher energy with decreasing fugacity of oxygen (Fig. 8c shows this shift for the NS3 composition). On the basis of the results shown in Figure 8c, molybdenum is then dominantly tetravalent in these sulfur-bearing glasses. When compared to polycrystalline molybdenite (MoS_2), the molybdenum K-edge XANES spectra for the sulfur-bearing glasses show large differences, suggesting that molybdenite did not nucleate in these glasses (the same conclusion is reached concerning the possibility that metallic molybdenum or crystalline sodium molybdate nucleated in the glasses). An amorphous variety of MoS_2 known as jordisite (Anthony *et al.* 1990) could correspond to the featureless XANES spectra for the glasses the richest in sulfur (Fig. 8) in Figure 8c. However, analysis of the EXAFS spectrum of this phase (based on Hibble & Wood 2004) rules out this model as this amorphous compound shows some Mo–Mo pairs, which are absent in our samples. Figures 9a and 9c show, respectively, the EXAFS spectra collected for these sulfur-bearing NS2 and NS3 glasses and their best-fit models. Their Fourier-Transforms (FT) are shown in Figures 9b and 9d, respectively. In these figures, the FT for the glasses are compared to those of crystalline sodium molybdate dihydrate and molybdenite model compounds. The FT show large differences among the samples, ranging from Mo–O environments in glasses synthesized at an
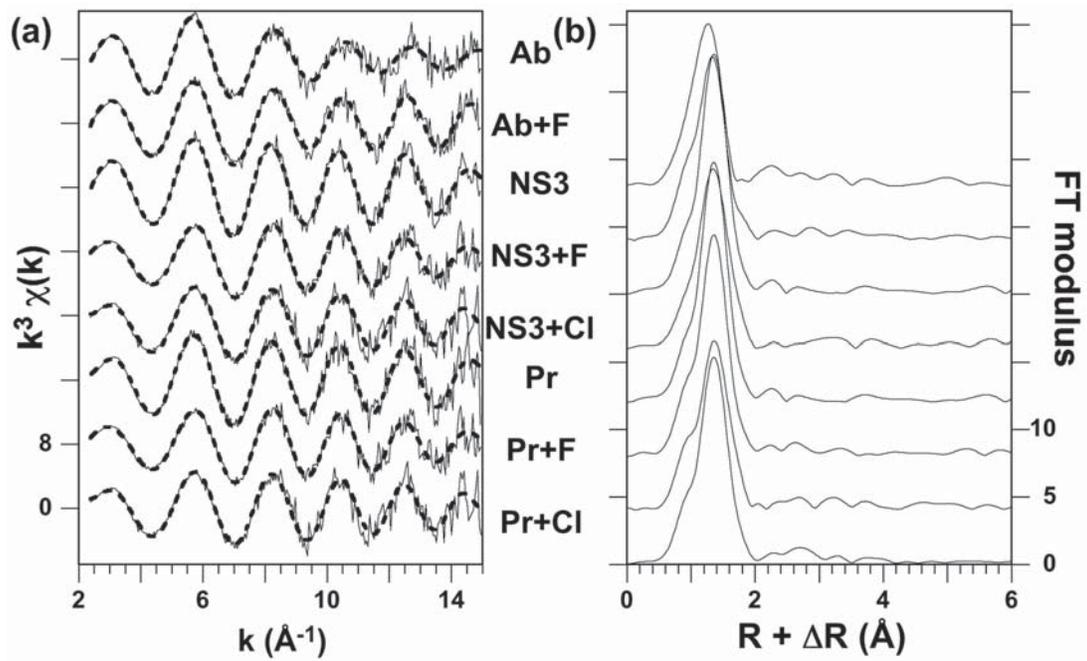
FIG. 7. Molybdenum K-edge-normalized, k^3-weighted EXAFS spectra (a) (solid: experimental; dotted: calculated model) and their corresponding Fourier transforms (b) for the glasses presented in Figure 5, confirming the weak influence of halogens on the coordination environment of Mo.
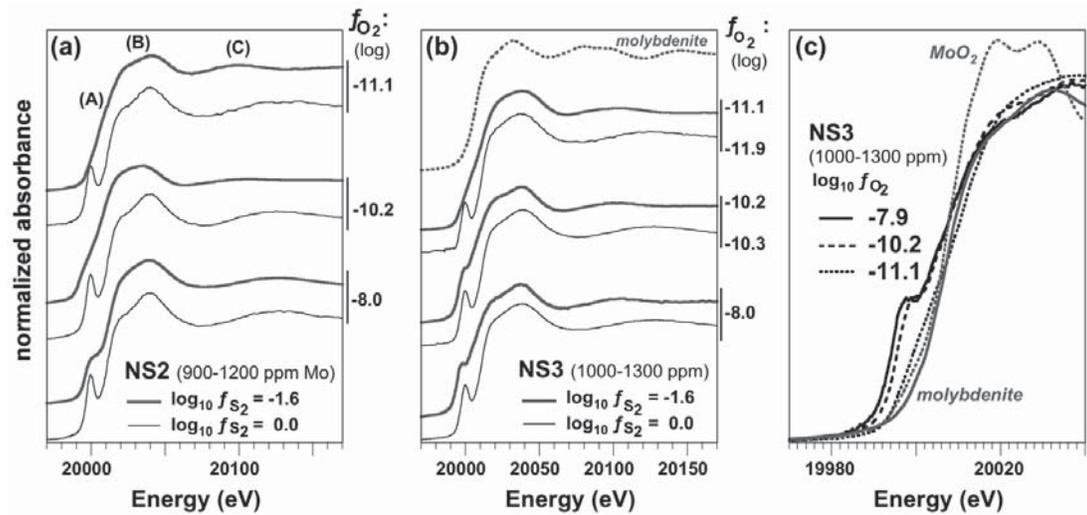

FIG. 8. (a) Molybdenum K-edge XANES spectra for sodium disilicate synthesized at various fugacities of oxygen and sulfur. (b) Same for sodium trisilicate glasses. (c) Overlapped XANES for sulfur-bearing NS3 glasses (synthesized at various conditions of oxygen fugacity) as compared to MoS_2 (molybdenite) and MoO_2 (tugarinovite) model compounds. Curves in black correspond to sulfur-free glasses, whereas those in gray are for the sulfur-bearing glasses. The XANES spectrum for molybdenite and MoO_2, showing large differences with respect to the XANES spectra of the glasses. The spectra for the glasses synthesized at 10^{-8} atm are taken from Farges *et al*. (2006), in which S-free glasses are discussed in detail.

oxygen fugacity of $10^{-8.0}$ atm (*i.e.*, near the magnetite–wüstite, MW, buffer) to Mo–O,S environments in the glasses prepared under more reducing conditions (between IW–1 and IW; see Table 1). Only sulfur first neighbors can result in the contributions located near 1.9 Å in the FT (this distance is uncorrected for phase shifts). This contribution cannot arise from first-neighbor molybdenum atoms, as the Mo–Mo distance would be too small in comparison to that for metallic molybdenum (~2.9 Å on the FT; see Fig. 5 in Farges *et al*. 2006). The presence of a mixed oxygen–sulfur first-neighbor environment around molybdenum in these

glasses was also demonstrated by a wavelet analysis of their EXAFS spectra (see Muñoz *et al*. 2003). EXAFS fits (Figs. 9a, c) of these environments in NS2 and NS3 glasses (Table 3) yielded 1.1–3.6 ± 0.05(5) atoms of oxygen at a distance from the absorbing molybdenum of 1.77(1) Å, which is characteristic of molybdate moieties, and 0–2.8(5) sulfur atoms within 2.13–2.18(1) Å (Table 3). These refined Mo–S distances are too short for Mo(IV)–S bonds (~2.39 Å as in molybdenite; Frondel & Wickman 1970). They are also too short to be consistent with those in jordisite (~2.30 Å, Hibble & Wood 2004).
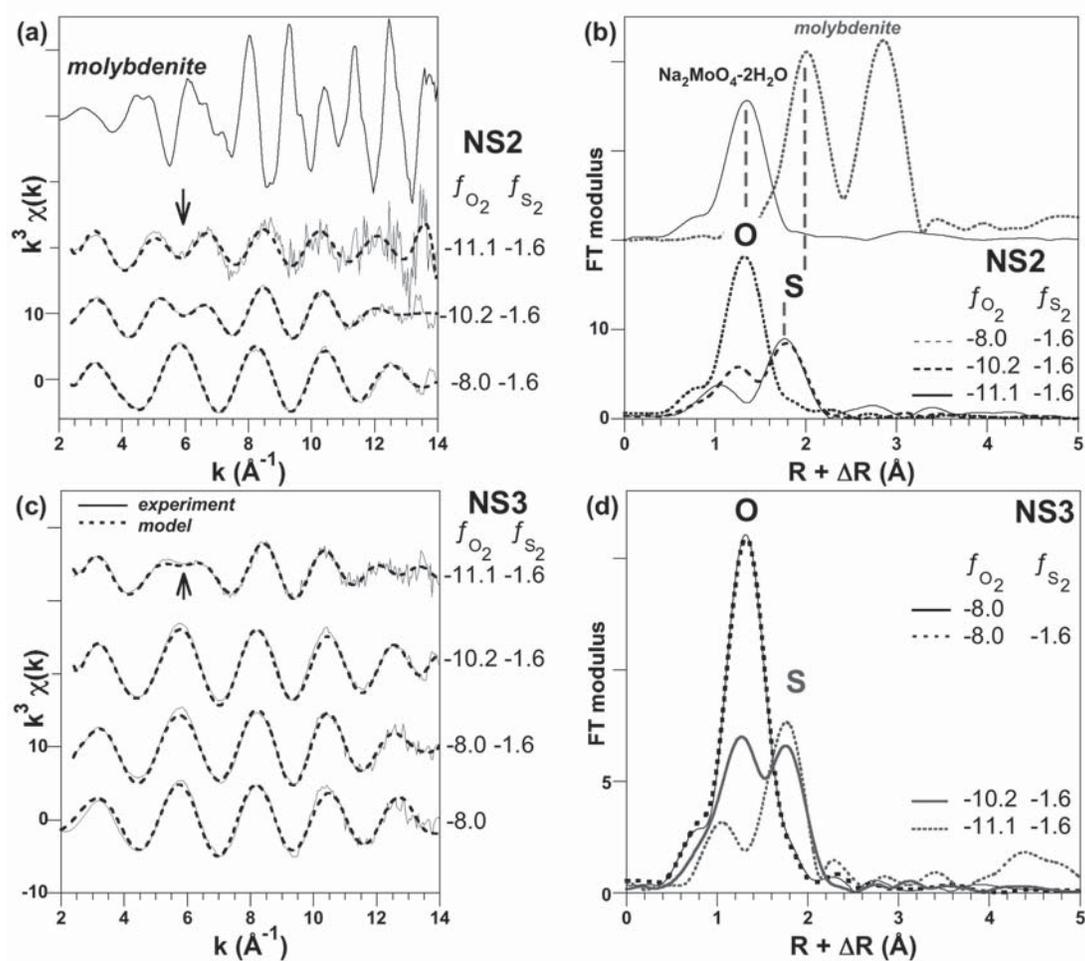

FIG. 9. Molybdenum K-edge-normalized, k^3-weighted EXAFS spectra (a,c) (solid: experimental; dotted: calculated model) and their corresponding Fourier-transforms (b, d) for the sulfur-bearing NS2 (top two figures) and NS3 glasses (bottom two figures), as compared to two model compounds (sodium molybdate dihydrate and molybdenite). Note the phase cancellation (arrows in Fig. 9a), which suggests the presence of thio-molybdate environments around molybdenum. Note the large increase in the magnitude of the Mo–S peak with decreasing fugacity of oxygen at a constant fugacity of sulfur, which does not get as high as the Mo–O peak for the molybdate moieties.

Evidence for Mo=S bonds within thio-oxo moieties

The short average Mo–S distances derived for the NS2,NS3 glasses are too short for Mo(IV)S$_4$ moeities, in which the average Mo–S distance is 2.3 Å. Another possibility is that molybdenum is hexavalent in these samples; however, this is not consistent with their molybdenum K-edge positions, which indicate Mo(IV). The most likely explanation for the short Mo–S distance and the Mo(IV) oxidation state is the presence of Mo(IV)=S bonds within a Mo(IV)S$_4^{4-}$ moiety [as known in (NH$_4$)$_2$MoS$_4$; Schaefer *et al.* 1977)]. In this compound, the average Mo–S distance is 2.17 Å, which is the same distance as in our glasses.

At an oxygen fugacity of 10^{-8} atm and 1650 K (~MW buffer), the presence (or the absence) of sulfur does not influence the speciation of molybdenum. However, below an oxygen fugacity of 10^{-10} atm and 1650 K (~IW buffer), sulfur progressively replaces oxygen first neighbors around molybdenum. Because XAFS spectroscopy averages over all configurations present in the glass, the mixed O,S-bearing environments observed in these glasses could be interpreted as indicating the presence of thio-oxo moieties (with variable O:S ratio) or a mixture of MoO$_n$ and MoS$_m$ moieties. However, a Principal Component Analysis (PCA) of the XANES and EXAFS spectra of the sulfur-bearing glasses indicates that two end-members (MoO$_n$ and MoS$_m$) could not be combined in variable amounts to produce the measured spectra. Also, there are no isobestic points (*i.e.*, points where all spectra converge in absorbance) if the XANES spectra of these glasses are plotted together (see NS3; Fig. 9c), which would be an additional indication of the presence of two end-members that are present in different concentrations in each glass. The PCA analysis therefore suggests that each of the NS2,NS3 glasses contain different species of molybdenum. In both compositions, the transition from first-shell environments around molybdenum consisting only of oxygen to various thio-oxo environments is sharp (within two log units in oxygen fugacity at most). We were not able to synthesize glasses at the lowest oxygen fugacities (below IW–3), so were not able to produce glasses with only sulfur as nearest neighbors (thio-moieities).

DISCUSSION

Influence of pressure and temperature on molybdenum speciation

The XANES and EXAFS spectra presented in this study show that molybdate moieties are not significantly affected by the pressure and temperature conditions considered (1 bar – 7 kbar, 295 to 1210 K) in the volatile-free glasses and melts under oxidizing conditions. The high bond-valence of the Mo–O bond in molybdate moieties (~1.5 valence units, *vu*; Farges

et al. 2006) makes these moieties relatively insensitive to moderate compression (due to pressure) or expansion (due to temperature). The predicted average linear thermal expansion for [4]Mo(VI)–O is ~2.7 × 10^{-6} K^{-1} (Hazen & Finger 1982), which is less than that for Si–O bonds (~4 × 10^{-6} K^{-1}). As a result, temperature-induced changes in coordination of molybdenum above T$_g$ are unlikely, at least in the range of temperatures investigated here. A similar statement can be made for the high-pressure glasses. The same reasoning can also apply to more reduced species of Mo. For example, the Mo(IV)–O bond in MoO$_6^{8-}$ coordination polyhedra has an average bond-valence of ~0.67 *vu*, and the average linear thermal expansion is predicted to be 6 × 10^{-6} K^{-1} (the same as zirconium in glass or melts under similar conditions of pressure and temperature; see Brown *et al.* 1995, Farges & Rossano 2000). Therefore, quenching is not expected to have a significant effect on the speciation of Mo(VI) or Mo(IV) in the relatively high-pressure silicate melts studied here, in agreement with the information on this speciation of zirconium in high-pressure silicate melts (Farges *et al.* 2006).

Effect of fluids on Mo speciation: bond-valence predictions

The presence of H$_2$O and halogens in the silicate glasses investigated in this study does not have a major effect on the speciation of molybdenum. Increased ordering of the local environments around molybdenum is the only significant modification induced by the presence of H$_2$O or halogens. Chlorine clearly does not "complex" molybdenum, nor does fluorine, on the basis of the evidence presented in this study. In silicate glasses and melts, chlorine cannot bond to [4]Mo(VI), because monovalent chlorine as first-neighbor anions can accept no more than one valence unit (±10%). Consequently, [4]Mo(VI) cannot be "complexed" by halogens if in tetrahedral coordination [in fluorides, Mo(VI) is always 6- (or more highly) coordinated]. We observed a poor affinity of molybdenum toward monovalent ligands, such as Cl and F, as compared to divalent ones such as oxygen and sulfur, and thus a similar weak affinity of molybdenum toward OH groups also is expected.

Where dissolved in polymerized silicate melts, H$_2$O forms hydroxyl groups and molecular H$_2$O, especially under H$_2$O-saturated conditions, as is the case for the glasses examined in this study; Kohn (2000), Liu *et al.* (2002), Mysen & Cody (2004) and Xue & Kanzaki (2004) reviewed this topic. These hydroxyl and molecular H$_2$O moieties are characterized by strong and weak hydrogen bonds, with bond valences of ~0.8 and 0.2 *vu*, respectively (Brown 1992). Molybdate moieties cannot bond directly to hydroxyl groups, as the sum of bond valences around the connecting atoms of oxygen (*i.e.*, 1.5 + 0.8 = 2.3 *vu*) would exceed by 0.3 *vu* the value required by Pauling's second rule for these atoms of

oxygen (2.0 ± 0.05 vu). However, some connections of molybdenum to oxygen atoms with more weakly bonded protons are plausible, as a replacement for some network modifiers in the medium-range environment of Mo(VI) (see proposed structural model at the top of Figure 12 in Farges *et al.* 2006). However, this topology is predicted to have only a minor influence on the thermodynamics of molybdenum in melts, as these "weak" bonds can recombine easily in the molten state. As a consequence, we have no experimental evidence that would support direct transport of molybdenum in the form of H_2O-, fluorine-, or chlorine-containing molybdenum moieties in the magmatic phase. Our findings for fluorine are in agreement with a number of indirect experiments on molybdenum partitioning between melts and fluids in the presence of fluorine (Isuk *et al.* 1983, 1984, Tingle & Fenn 1982, Keppler & Wyllie 1990). In contrast, sulfur forms direct bonds with molybdenum and is thus likely to play a direct role in the transport of molybdenum in the magma-hydrothermal systems, as discussed below.

The role of sulfur in molybdenum speciation

The speciation of sulfur in geological glasses has been investigated in a number of studies, including those by Nagashima & Katsura (1973), Katsura & Nagashima (1974), Carroll & Rutherford (1985, 1988), Nilsson & Peach (1993), Carroll & Webster (1994), Wallace & Carmichael (1992, 1994), Moretti & Ottonello (2002), and Tsujimura *et al.* (2004). Métrich & Clocchiatti (1996) conducted the first sulfur-K edge XANES experiments on natural glasses, followed by Paris *et al.* (2002). These authors showed that in silicate glasses of geological interest, sulfur occurs predominantly as SO_4^{2-} and S^{2-} (depending on oxygen fugacity), with no evidence for more than 5% of intermediate oxidation states of sulfur, such as S^{4-} (*i.e.,* sulfites) (Métrich *et al.* 2002, 2003). On the basis of this information, and given the amounts of dissolved sulfur in our glasses, sulfur is present dominantly as sulfide moieties in our glasses because of the relatively low oxygen fugacity conditions under which they were synthesized (QFM–IW buffers). However, one cannot exclude the possibility of trace amounts of more oxidized sulfur in our glasses, as XANES is not sensitive where a particular oxidation state of sulfur is too dilute. Therefore, an attempt to measure the speciation of sulfur in our samples would not have been very conclusive with regard to the trace amounts of molybdenum probed by molybdenum K-edge XAFS methods.

We observed that sulfur (as S^{2-}) "complexes" molybdenum efficiently if both the oxygen fugacity drops below QFM and the sulfur fugacity increases to produce sulfide groups (S^{2-}). Also, the lack of second neighbors in the FT of sulfur-rich, reduced, molybdenum-bearing glasses (Figs. 9b, d) suggests that molybdenum is not directly connected to the network of tetrahedra, which is likely to be a consequence of short Mo(IV)=S bonds. The bond valence of such bonds is very high (~1.7 vu based on O'Keeffe & Brese 1992). As is the case for molybdates, these (Mo=S)-bearing units cannot bond to oxygen atoms connected to other highly charged cations, such as the network formers $^{IV}Si(IV)$ and $^{IV}Al(III)$. Because of these bonding constraints, we suggest that Mo=S moieties can be efficiently removed by fluids from the melt. On the basis of similar arguments, molybdate moieties can also be easily "extracted" from supercooled melts by nucleation processes, such as in powellite, $CaMoO_4$ (see Farges *et al.* 2006). In this context, sulfur acts indirectly as an efficient vector for molybdenum transport in agreement with its chalcophilic character (Tingle & Fenn 1982). However, the ability of sulfur to facilitate the transport of molybdenum and its partitioning into the fluid phase is an indirect effect, as it is the formation of Mo=S bonds in the melt that results in molybdenum being disconnected from the framework of tetrahedra.

First evidence for thio-oxo moieties in geochemical oxide glasses

On the basis of a principal component analysis, we found that the local environment around molybdenum cannot be described with a simple mixture of molybdenum oxide and molybdenum sulfide species in the sulfur-bearing oxide glasses studied. Instead, the oxygen ligands around molybdenum are progressively replaced by sulfur first neighbors, as oxygen fugacity is lowered, while the sulfur fugacity is kept constant. This finding suggests that molybdenum is reduced progressively from a hexavalent to a tetravalent oxidation state with variable numbers of oxygen and sulfur ligands. Molybdenum sulfite-oxidase and thio-oxo-type compounds (also known as thio-molybdates; see McMaster *et al.* 2001) provide an example of this property of molybdenum. Among these compounds, $Cs_2Mo(VI)OS_3$ (Krebs *et al.* 1970) is the closest model we found that is representative of the short-range local structure of molybdenum in sulfur-bearing NS2,NS3 glasses synthesized at an $f(O_2)$ of 10^{-10} atm. In Cs_2MoOS_3, Mo(VI) is surrounded by one oxygen atom at 1.78 Å (molybdate-like) and three sulfur ligands at 2.18 Å (T_d geometry). Next-nearest neighbors include Cs atoms at distances between 4 and 4.3 Å, confirming that the $Mo(VI)OS_3^{2-}$ moieties are charge-compensated only by network modifiers in this compound. This compound belongs to a family of thio-molybdates, in which the molybdate moieties [$Mo(VI)O_4^{2-}$ units *sensu stricto*] are replaced progressively by "thio-molybdenyl" moieties, [$(Mo(VI,V,IV)=O)S_3^{n-}$. At higher fugacities of sulfur, these thio-molybdenyl units can be replaced by [$Mo(IV)S^{2-}_4]^{2-}$ moieties, as in the isostructural $(NH_4)_2Mo(IV)S_4$ (Schaefer *et al.* 1977) or Rb_2MoS_4 (Ellermeier *et al.* 1999). In $(NH_4)_2MoS_4$, molybdenum is surrounded by four sulfur atoms near

2.16–2.20 Å, and no molybdenyl bond is present (Schaefer *et al*. 1977).

Thiomolybdates are known in molybdenum-bearing sulfide-rich waters such as those of the Black Sea (Erikson & Helz 2000). This family of compounds is characterized by the generic formula $Mo(VI)O_n S_{4-n}^{2-}$ with $n = 1$, 2 or 3 (thio-, trithio- and tetrathio-oxo, respectively). Their optical absorption spectra show various intense transitions in the near-UV region (between 275 and 550 nm; Erikson & Helz 2000), which is consistent with the yellowish color of the sulfur-bearing glasses synthesized in this study. Hence, on the basis of EXAFS results and the above information, we conclude that our molybdenum- and sulfur-bearing NS2 and NS3 glasses most likely contain thio-, dithio-, trithio-, and tetrathio-oxo moieties. This suggestion helps to explain why the number of sulfur first neighbors around molybdenum increases if the fugacity of oxygen decreases (at a constant sulfur fugacity of $10^{-1.6}$ atm). This observation is also consistent with the polymerization of molybdenum (as known in these thio-oxo compounds), which increases with decreasing fugacity of oxygen. For example, as oxygen fugacity decreases, $[Mo(VI)S^{2-}_4]^{2-}$ moieties are replaced by $[Mo(V)S^{2-}_8]^{11-}$ dimeric moieties, as in $(NH_4)_2(Mo_2S_{12})$ (Wignacourt *et al*. 1992), in which the charge-compensating behavior of network modifiers becomes less and less prominent as a result of the polymerization of molybdenum. At even lower fugacity of oxygen, only a few network modifiers are required around the central $Mo(IV)$ [as in $(NH_4)_2MoS_4$; Schaefer *et al*. 1977]. Finally, in the absence of available network-modifiers (as is the case where molybdenum is extracted from the melt phase by fluids, for example), $Mo(IV)$ must polymerize (as outlined above), and consequently the Mo–X bonds must decrease their bond valence (otherwise, the polymerization cannot occur). Consequently, highly coordinated $Mo(IV)$–S environments must form, namely $Mo(IV)S_6^{8-}$ units (as in molybdenite). The same behavior occurs where MoO_3 nucleates from a molybdate-bearing, fully polymerized melt (*i.e.,* where "MoO_3 saturation" occurs; see Ryabchikov *et al*. 1981).

Geochemical implications

The absence of local structural environments around molybdenum similar to those in molybdenite in any of the glasses studied here is striking because molybdenite is the most abundant molybdenum-containing mineral in magmatic systems. However, it is now well documented that the molecular-level speciation of many high-field-strength elements (such as titanium, zirconium, niobium, and tin in glasses and melts; see Farges *et al*. 1991, Ellison 1994, Ellison & Hess 1994, Hess 1995, Brown *et al*. 1995, Marr 1998, Piilonen *et al*. 2005) is generally at variance with their local structural environments in the dominant minerals in which they occur in igneous systems. For example, the local environment of zirconium in silicate glasses and melts is closer to that in alkali zirconosilicates than in zircon; tin has a local environment more like that in eakerite than in cassiterite in melts, and titanium has a local environment more like that in fresnoite than in rutile in melts. In addition, the influence of late fluids in natural magmatic-hydrothermal systems may enhance the differences between our spectroscopic observations and geochemical observations (see Isuk & Carman 1981, 1983, 1984, Candela & Holland 1984, Keppler & Wyllie 1990, Schäfer *et al*. 1999).

Our results indicate that molybdenum can adapt to a variety of local structural environments, in which the exchange of highly covalent oxygen ligands by double-bonded sulfur ligands is progressive. This exchange of ligands occurs as the sulfur fugacity increases and molybdenum is reduced to its tetravalent oxidation state (near the IW buffer). In parallel, as the fugacity of oxygen decreases, the oxidation state of molybdenum also can decrease, with concomitant changes in the local coordination-environment of molybdenum (including various thio-molybdate environments with different O:S ratios and with double-bonded S^{2-}). As the oxygen fugacity decreases, fewer network-modifiers are required around the central molybdenum atoms as a result of a lower oxidation state of molybdenum. As a result, molybdenum is increasingly polymerized and "complexed" by sulfide ligands through double bonds, which makes these thioxo (ranging from monothio-oxo to tetrathio-oxo) units highly mobile within the framework of tetrahedra in the melt. As a result of this speciation, partitioning of molybdenum-thio-oxo moieties into an exsolved fluid phase should be a lower-energy process, which helps explain the large melt–fluid partitioning coefficients of molybdenum observed during melt–H_2O vapor experiments (Tingle & Fenn 1982, 1984). In addition, Ryabchikov *et al*. (1981) showed that saturation with respect to the molybdenite component occurs as the coexisting highly polymerized, sulfur-free melt becomes saturated with respect to molybdite (MoO_3). Accordingly, late hydrothermal fluids appear to play a key role in the final stage of the transport of molybdenum in the form of $Mo(IV)S_4^{4-}$ moieties. Such partitioning could possibly be initiated during the magmatic stage, when molybdenum has a mixed O–S ligand shell, in agreement with Hattori *et al*. (2002). Direct *in situ* spectroscopic experiments under supercritical conditions would be required to test this model.

Finally, we stress the importance of studying glasses and melts containing a variety of volatiles (particularly sulfur for siderophile and chalcophile elements) to build more robust models for the speciation and transport properties of transition elements in geochemical systems. This study of molybdenum in silicate melts and glasses shows how the effects of such volatiles on molybdenum speciation and partitioning can be fairly complex and indirect. Once more, a combination of

spectroscopies reveals that silicate melts are characterized by a variety of unusual environments with regard to the most common mineral phases crystallizing from these melts. Our findings highlight the utility of transferring molecular-level information on transition-metal speciation from aqueous geochemistry to melt geochemistry, which in this case led to the conclusion that unexpected new sulfur-bearing species can form and have a major effect on the way chalcophile elements are transported in fluid-rich, late-stage magmas, and reconciled structural information for generic oxide glasses to geochemical lines of evidence.

REFERENCES

ANTHONY, J., BIDEAUX, R., BLADH, K. & NICHOLS, M. (1990): *Handbook of Mineralogy*. **1**. *Elements, Sulfides, Sulfosalts*. Mineral Data Publishing, Tucson, Arizona.

AZIF, E. (1998): *Solubilité des éléments du groupe du platine (Pt et Pd) dans les liquides silicatés en fonction de la fugacité d'oxygène, de soufre, de la température, de la pression et de la composition. Expérimentation, modélisation, implications métallogéniques et géochimiques*. Ph.D. thesis, Université d' Orléans, Orléans, France.

BAI, T.B. & KOSTER VAN GROOS, A.F. (1999): The distribution of Na, K, Rb, Sr, Al, Ge, Cu, W, Mo, La, and Ce between granitic melts and coexisting aqueous fluids. *Geochim. Cosmochim. Acta* **63**, 1117-1131.

BENDOR, L. & SHIMONY, Y. (1974): Crystal-structure, magnetic-susceptibility and electrical-conductivity of pure and NiO-doped MoO_2 and WO_2. *Mater. Res. Bull.* **9**, 837-844.

BENSIMON, Y., BELOUGNE, P., DEROIDE, B., DUCOURANT, B., GIUNTINI, J.C. & ZANCHETTA, J.V. (1991): Influence of oxygen on electrical-conductivity of amorphous molybdenum sulfides. *J. Non-Crystal. Solids* **134**, 239-248.

BERNDT, J., LIEBSKE, C., HOLTZ, F., FREISE, M., NOWAK, M., ZIEGENBEIN, D., HURCKUCK, W. & KOEPKE, J. (2002): A combined rapid-quench and H_2-membrane setup for internally heated pressure vessels: description and application for water solubility in basaltic melts. *Am. Mineral.* **87**, 1717-1726.

BERRY, A.J., SHELLEY, J.M.G., FORAN, G.J., O'NEILL, H.S.C. & SCOTT, D.R. (2003): A furnace design for XANES spectroscopy of silicate melts under controlled oxygen fugacities and temperatures to 1773K. *J. Synchrotron Rad.* **10**, 332-336.

BOOKSTROM, A.A. (1999): Molybdenum. *In* The Encyclopedia of Geochemistry (C. Marshall & R.W. Fairbridge, eds.). Chapman and Hall, New York, N.Y. (412-413).

BROWN, G.E., JR., FARGES, F. & CALAS, G. (1995): X-ray scattering and spectroscopy studies of molten silicates. *In* Structure, Dynamics, and Properties of Silicate Melts (J.F. Stebbins, D.B. Dingwell & P.F. McMillan, eds.). *Rev. Mineral.* **32**, 317-408.

BROWN, I.D. (1992): Chemical and steric constraints in inorganic solids. *Acta Crystallogr.* **B48**, 553-572.

CANDELA, P.A. & HOLLAND, H.D. (1984): The partitioning of Cu and Mo between silicate melts and aqueous fluids. *Geochim. Cosmochim. Acta* **48**, 373-380.

CANDELA, P.A. & HOLLAND, H.D. (1986): A mass transfer model for copper and molybdenum in magmatic hydrothermal systems: origin of the porphyry-type ore deposit. *Econ. Geol.* **81**, 1-19.

CARROLL, M.R. & RUTHERFORD, M.J. (1985): Sulfide and sulfate saturation in hydrous silicate melts. *J. Geophys. Res.* **90**, C601–C612.

CARROLL, M.R. & RUTHERFORD, M.J. (1988): Sulfur speciation in hydrous experimental glasses of varying oxidation state: results from measured wavelength shifts of sulfur X-rays. *Am. Mineral.* **73**, 845-849.

CARROLL, M.R. & WEBSTER, J.D. (1994): Solubilities of sulfur, noble gases, nitrogen, chlorine, and fluorine in magmas. *In* Volatiles in Magmas (M.R. Carroll & J. Holloway, eds.). *Rev. Mineral.* **30**, 231-279.

CARTEN, R.B., WHITE, W.H. & STERN, H.J. (1993): High-grade granite-related molybdenum systems: classification and origins. *In* Mineral Deposit Modeling (R.V. Kirkham *et al.*, eds.). *Geol. Assoc. Can., Spec. Pap.* **40**, 521-554.

CHEVYCHELOV, V.YU. & CHEVYCHELOVA, T.K. (1997): Partitioning of Pb, Zn, W, Mo, Cl, and major elements between aqueous fluid and melt in the systems granodiorite (granite, leucogranite)-H_2O–NaCl–HCl. *Neues Jahrb. Mineral. Abh.* **172**, 101-115.

COTTON, F.A. & WILKINSON, G. (1988): *Advanced Inorganic Chemistry*. J. Wiley & Sons, New York., N.Y.

CROZIER, E.D., REHR, J.J. & INGALLS, R. (1988): Amorphous and liquid systems. *In* X-Ray Absorption. Principles, Applications, Techniques of EXAFS, SEXAFS and XANES (D.C. Koningsberger & R. Prins, eds.). John Wiley, New York, N.Y. (373-442).

ELLERMEIER, J, NAETHER, C. & BENSCH, W. (1999): Dirubidium tetrasulfidomolybdate, $Rb_2(MoS_4)$. *Acta Crystallogr.* **C55**, 1748-1751.

ELLISON, A.J.G. (1994): "Charge-balance" of Zr^{4+} in K_2O–ZrO_2–SiO_2 glasses. *Trans. Am. Geophys. Union* (*Eos*) **75**, 714 (abstr.).

ELLISON, A.J.G. & HESS, P.C. (1994): Raman study of potassium silicate glasses containing Rb^+, Sr^{2+}, Y^{3+}, and Zr^{4+}: implications for cation solution mechanisms in multicomponent silicate liquids. *Geochim. Cosmochim. Acta* **58**, 1877-1887.

ERICKSON, B.E. & HELZ, G.R. (2000): Molybdenum(VI) speciation in sulfidic waters; stability and lability of thiomolybdates. *Geochim. Cosmochim. Acta* **64**, 1149-1158.

FARGES, F. (1991): Structural environment around Th^{4+} in silicate glasses. Implications for the geochemistry of incompatible Me^{4+} elements. *Geochim. Cosmochim. Acta* **55**, 3303-3319.

FARGES, F., BROWN, G.E., JR., CALAS, G., GALOISY, L. & WAYCHUNAS, G.A. (1994): Structural transformation in Ni-bearing $Na_2Si_2O_5$ glass and melt. *Geophys. Res. Lett.* **21**, 1931-1934.

FARGES, F., BROWN, G.E., JR., NAVROTSKY, A., GAN, H. & REHR, J.J. (1996): Coordination chemistry of Ti(IV) in silicate glasses and melts. III. Glasses and melts between 293 and 1650 K. *Geochim. Cosmochim. Acta* **60**, 3055-3065.

FARGES, F., DJANARTHANY, S., DE WISPELAERE, S., MUÑOZ, M., WILKE, M., SCHMIDT, C., BORCHERT, M., TROCELLIER, P., CRICHTON, W., SIMIONOVICI, A., PETIT, P.-E., MEZOUARD, M., ETCHEVERRY, M.-P. & PALLOT-FROSSARD, I. (2005b): Water in silicate glasses and melts of environmental interest: from volcanoes to cathedrals. *Phys. Chem. Glasses* (*in press*).

FARGES, F., MUÑOZ, M., SIEWERT, R., MALAVERGNE, V., BROWN, G.E., JR., BEHRENS, H., NOWAK, M. & PETIT, P.-E. (2001): Transition elements in water-bearing silicate glasses/melts. II. Ni in water-bearing glasses. *Geochim. Cosmochim. Acta* **86**, 1679-1693.

FARGES, F., PONADER, C.W. & BROWN, G.E., JR. (1991): Local environment around incompatible elements in silicate glass/melt systems. I. Zr at trace levels. *Geochim. Cosmochim. Acta* **55**, 1563-1574.

FARGES, F., PONADER, C.W., CALAS, G. & BROWN, G.E., JR. (1992): Local environment around incompatible elements in silicate glass/melt systems. II. U(VI), U(V) and U(IV). *Geochim. Cosmochim. Acta* **56**, 4205-4220.

FARGES, F. & ROSSANO, S. (2000): Water in Zr-bearing synthetic and natural glasses. *Eur. J. Mineral.* **12**, 1093-1107.

FARGES, F., SHARPS, J.A. & BROWN, G.E., JR. (1993): Local environment around gold(III) in aqueous chloride solutions: an EXAFS spectroscopy study. *Geochim. Cosmochim Acta* **57**, 1243-1252.

FARGES, F., SIEWERT, R., BROWN, G.E., JR., GUESDON, A. & MORIN, G. (2005a): Structural environments around molybdenum in silicate glasses and melts. I. Influence of composition and oxygen fugacity on the local structure of molybdenum. *Can. Mineral.* **44**,

FRONDEL, J.W. & WICKMAN, F.E. (1970): Molybdenite polytypes in theory and occurrence. II. Some naturally-occurring polytypes of molybdenite. *Am. Mineral.* **55**, 1857-1875.

HATTORI, K.H., DE HOOG, J.C.M. & KEITH, J.D. (2002): Role of oxidized, sulfur-rich mafic magmas for porphyry copper mineralization. *Geol. Soc. Am., Abstr. Programs* **34**, 88.

HAZEN, R.M. & FINGER, L.W. (1982): *Comparative Crystal Chemistry. Temperature, Pressure, Composition and the Variation of Crystal Structure*. John Wiley & Sons, New York, N.Y.

HESS, P.C. (1995): Thermodynamic mixing properties and the structure of silicate melts. *In* Structure, Dynamics, and Properties of Silicate Melts (J.F. Stebbins, D.B. Dingwell & P.F. McMillan, eds.). *Rev. Mineral.* **32**, 147-189.

HIBBLE, S.J. & WOOD, G.B. (2004): Modeling the structure of amorphous MoS_3: a neutron diffraction and reverse Monte Carlo study. *J. Am. Chem. Soc.* **126**, 959-965.

HOLZHEID, A., BORISOV, A. & PALME, H. (1994): The effect of oxygen fugacity and temperature on solubilities of nickel, cobalt, and molybdenum in silicate melts. *Geochim. Cosmochim. Acta* **58**, 1975-1981.

HORNG, T. (1999): The interactions between M^{+5} cations (Nb^{+5}, Ta^{+5} or P^{+5}) and anhydrous haplogranite melts. *Geochim. Cosmochim. Acta* **63**, 2419-2428.

ISUK, E.E. & CARMAN, J.H. (1981): The system $Na_2Si_2O_5$–$K_2Si_2O_5$–MoS_2–H_2O with implications for molybdenum transport in silicate melts. *Econ. Geol.* **76**, 2222-2235.

ISUK, E.E. & CARMAN, J.H. (1983): Behavior of molybdenum in alkali silicate melts; effects of excess SiO_2 and CO_2. *Lithos* **16**, 17-22.

ISUK, E.E. & CARMAN, J.H. (1984): Transport and concentration of molybdenum in granite molybdenite systems; effects of fluorine and sulfur; discussion and reply. *Geology* **12**, 568-569.

JACKSON, W.E., BROWN, G.E., JR., WAYCHUNAS, G.A., MUSTRE DE LEON, J., CONRADSON, S. & COMBES, J.-M. (1993): High-temperature XAS study of Fe_2SiO_4: evidence for reduced coordination of ferrous iron in the liquid. *Science* **262**, 229-233.

KATSURA, T. & NAGASHIMA, S. (1974): Solubility of sulfur in some magmas at 1 atm pressure. *Geochim. Cosmochim. Acta* **38**, 517-531.

KEPPLER, H. & WYLLIE, P.J. (1990): Role of fluids in transport and fractionation of uranium and thorium in magmatic processes. *Nature* **348**, 531-533.

KOHN, S.C. (2000): The dissolution mechanisms of water in silicate melts; a synthesis of recent data. *Mineral. Mag.* **54**, 181-200.

KRAUSE, M.O. & OLIVER, J.H. (1979): Natural widths of atomic *K* and *L* levels, *K*α X-ray lines and several *KLL* Auger lines. *J. Phys. Chem. Ref. Data* **8**, 329-338.

KRAVCHUK, I.F., MALININ, S.D., SENIN, V.G. & DERNOV-PEGAREV, V.F. (2000): Molybdenum partition between melts of natural and synthetic aluminosilicates and aqueous-salt fluids. *Geochem. Int.* **38**, 130-137.

KREBS, B., MUELLER, A. & KINDLER, E. (1970): Kristall-struktur von Cs_2MoOS_3. *Z. Naturforsch. (Teil B. Anorg. Chemie, Org. Chemie)* **25**, 222.

LINNEN, R.L. (1998): Depth of emplacement, fluid provenance and metallogeny in granitic terrains: a comparison of western Thailand with other Sn–W belts. *Mineral. Deposita* **33**, 461-476.

LIU, Y., NEKVASIL, H. & LONG, H. (2002): Water dissolution in albite melts: constraints from ab initio NMR calculations. *Geochim. Cosmochim. Acta* **66**, 4149-4163.

MARR, R.A. (1998): *An Investigation of Zr and Ti-Bearing Alkali Aluminosilicate Glasses; Solubility Experiments, Raman Spectroscopy and ^{23}Na NMR Analyses*. Ph.D. thesis, McGill Univ., Montreal, Quebec.

MCMASTER, J., CARDUCCI, M.D., YANG, Y.-S., ENEMARK, J.H. & SOLOMON, E.I. (2001): Electronic spectral studies of molybdenyl complexes. II. MCD spectroscopy of $[MoOS_4]$ centers. *Inorg. Chem.* **40**, 687-702.

MÉTRICH, N., BONNIN-MOSBAH, M., SUSINI, J., MENEZ, B. & GALOISY, L. (2002): Presence of sulfite (S–IV) in arc magmas: implications for volcanic sulfur emission. *Geophys. Res. Lett.* **29**, doi:10.1029/ 2001GL014607.

METRICH, N. & CLOCCHIATTI, R. (1996) Sulfur abundance and its speciation in primitive oxidized alkaline melts. *Geochim. Cosmochim. Acta* **60**, 4151-4160.

MÉTRICH, N., SUSINI, J., GALOISY, L., CALAS, G., BONNIN-MOSBAH, M. & MENEZ, B. (2003): X-ray microspectroscopy of sulfur in basaltic glass inclusions. Inference on the volcanic sulfur emissions. *J. Phys. IV* **104**, 393-397.

MORETTI, R. & OTTONELLO, G. (2002) The solubility and speciation of sulfur in silicate melts; development of the conjugated Toop-Samis-Flood-Grjotheim (CTSFG) model. *Geochim. Cosmochim. Acta* **66**, 524.

MUÑOZ, M., ARGOUL, P. & FARGES, F. (2003): Continuous Cauchy wavelet transform analyses of EXAFS spectra: a qualitative approach. *Am. Mineral.* **88**, 694-700.

MYSEN, B.O. & CODY, G.D. (2004): Solubility and solution mechanism of H_2O in alkali silicate melts and glasses at high pressure and temperature. *Geochim. Cosmochim. Acta* **68**, 5113–5126.

NAGASHIMA, S. & KATSURA, T. (1973): The solubility of sulfur in $Na_2O–SiO_2$ melts under various oxygen partial pressures. *Bull. Chem. Soc. Japan* **46**, 3099-3103.

NILSSON, K. & PEACH, C.L. (1993): Sulfur speciation, oxidation state and sulfur concentrations in back arc magmas. *Geochim. Cosmochim. Acta* **57**, 3807-3813.

O'KEEFFE, M. & BRESE, N.E. (1992): Bond valence parameters for anion–anion bonds in solids. *Acta Crystallogr.* **B48**, 152-154.

O'NEILL, H.S.C. & EGGINS, S.M. (2002) The effect of melt composition on trace element partitioning: an experimental investigation of the activity coefficients of FeO, NiO, CoO, MoO_2 and MoO_3 in silicate melts. *Chem. Geol.* **186**, 151-181.

OZEKI, T., ADACHI, H. & SHIGERO, I. (1996): Estimation of the dissolved structures and condensation reactivities of mononuclear molybdenum(VI) species in solution using the UV-vis absorption spectra and molecular orbital calculation DV-Xα. *Bull. Chem. Soc. Japan* **69**, 619-625.

PARIS, E., DINGWELL, D.B., SEIFERT, F.A., MOTTANA, A. & ROMANO, C. (1994): Pressure-induced coordination change of Ti in silicate glass: a XANES study. *Phys. Chem. Minerals* **21**, 510-515.

PARIS, E., GIULI, G., CARROLL, M.R. & DAVOLI, I. (2002): The valence and speciation of sulfur in glasses by X-ray absorption spectroscopy. *Can. Mineral.* **39**, 331-339.

PIILONEN, P., FARGES, F., LINNEN, R. & BROWN, G.E., JR. (2005): Sn and Nb in dry and fluid-rich (H_2O, F) silicate glasses. *Phys. Scripta* T**115**, 405-407.

PONADER, C.W. & BROWN, G.E., JR. (1989a): Rare earth elements in silicate glass/melt systems. I. Effects of composition on the coordination environments of La, Gd, and Yb. *Geochim. Cosmochim. Acta* **53**, 2893-2903.

PONADER, C.W. & BROWN, G.E., JR. (1989b): Rare earth elements in silicate glass/melt systems. II. Interactions of La, Gd, and Yb with halogens. *Geochim. Cosmochim. Acta* **53**, 2905-2914.

RYABCHIKOV, I.D., REKHARSKY, V.I. & KUDRIN, A.V. (1981): Mobilization of molybdenum by magmatic fluids in the process of crystallization of granite melt. *Geokhimiya*, 1243-1246.

SALOVA, T.P., ORLOVA, G.P., KRAVCHUK, I.P., EPEL'BAUM, M.B., RYABCHIKOV, I.D. & MALININ, S.D. (1989): The problem of experimental determination of molybdenum partitioning coefficients between silicate melt and water–salt fluid. *Geokhimiya* **2**, 267-273.

SCHÄFER, B., FRISCHKNECHT, R., GÜNTHER, D.B. & DINGWELL, D.B. (1999): Determination of trace-element partitioning between fluid and melt using LA–ICP–MS analysis of synthetic fluid inclusions in glass. *Eur. J. Mineral.* **11**, 415-426.

SCHAEFER, H., SCHAEFER, G & WEISS, A. (1977): Zur Kristall-struktur von Ammoniumtetrathio-molybdat *Z. Naturforsch. B (Anorg. Chemie, Organ. Chemie)* **19**, 76.

SEEDORFF, E. & EINAUDI, M.T. (2004) Henderson porphyry molybdenum system, Colorado. II. Decoupling of intro-duction and deposition of metals during geochemical evo-lution of hydrothermal fluids. *Econ. Geol.* **99**, 39-72.

SHANNON, R.D. & PREWITT, C.T. (1969): Effective ionic radii in oxides and fluorides. *Acta Crystallogr.* **B25**, 925-945.

TINGLE, T.N. & FENN, P.M. (1982): Concentration and trans-port of molybdenum in magmatic systems: the effects of fluorine and sulphur. *Trans. Am. Geophys. Union* (Eos) xx, V81C-21 (abstr.).

TINGLE, T.N. & FENN, P.M. (1984): Transport and concentra-tion of molybdenum in granite molybenite systems: effect of fluorine and sulfur. *Geology* **12**, 156-158.

TSUJIMURA, T., XUE, X., KANZAKI, M. & WALTER, M.J. (2004): Sulfur speciation and network structural changes in sodium silicate glasses: constraints from NMR and Raman spec-troscopy. *Geochim. Cosmochim. Acta* **68**, 5081-5101.

WALLACE, P. & CARMICHAEL, I.S.E. (1992): Sulfur in basaltic magmas. *Geochim. Cosmochim. Acta* **56**, 1863-1874.

WALLACE, P. & CARMICHAEL, I.S.E. (1994): S speciation in submarine basaltic glasses as determined by measure-ments of S Kα X-ray wavelength shifts. *Am. Mineral.* **79**, 161-167.

WALTER, M.J. & THIBAULT, Y. (1995) Partitioning of tungsten and molybdenum between metallic liquid and silicate melt. *Science* **270**, 1186-1189.

WAYCHUNAS, G.A., BROWN, G.E., JR., PONADER, C.W. & JACKSON, W.E. (1988): Evidence from x-ray absorption for network-forming Fe^{2+} in molten alkali silicates. *Nature* **332**, 251-253.

WEBSTER, J.D. (1999): Exsolution of magmatic volatile phases from Cl-enriched mineralizing granitic magmas and impli-cations for ore metal transport. *Geochim. Cosmochim. Acta* **61**, 1017-1029.

WHITE, W.H., BOOKSTROM, A.A., KAMILLI, R.J., GANSTER, M.W., SMITH, R.P., RANTA, D.E. & STEININGER, R.C. (1981): Character and origin of Climax-type molybdenum deposits. *Econ. Geol.* **75**, 270-316.

WIGNACOURT, J.P., DRACHE, M., SWINNEA, J.S., STEINFINK, H., LORRIAUX-RUBBENS, A. & WALLART, F. (1992): Crystal structure and Raman scattering investigation of anhydrous $(NH_4)_2(Mo_2S_{12})$. *Can. J. Appl. Spectrosc.* **37**, 49-54.

WILKE, M. & BEHRENS, H. (1999): The use of iron partitioning between plagioclase and melt as an oxygen barometer for hydrous magmatic systems. *Terra Nova* **11**, *suppl.* 1.

WINTERER, M. (1997): The XAFS package. *J. Phys. IV, Colloq.* **7-C2**, 243-244.

XUE, X. & KANZAKI, M. (2004): Dissolution mechanisms of water in depolymerized silicate melts: constraints from ^1H and ^{29}Si NMR spectroscopy and ab initio calculations. *Geochim. Cosmochim. Acta* **68**, 5027–5057.